

Characterization of Semi-insulating GaAs for Detector Fabrication

J. W. Chen ^{1,2}, D. Ebling ², C. Eiche ³, M. Fiederle ², T. Frömmichen ¹, P. Hug ¹, R. Irsigler ¹, W. Jantz ⁴, J. Ludwig ¹, T. Plötze ¹, M. Rogalla ¹, K. Runge ^{1,2}, R. Stibal ⁴

¹University of Freiburg, Faculty of Physics, Germany

²Freiburg Materials Research Center (FMF), Germany

³Kristallographisches Institut Freiburg, Germany

⁴Fraunhofer Institut für angewandte Festkörperphysik (IAF), Freiburg, Germany

1 Abstract

Radiation detectors work as Schottky devices. The Schottky contact of the investigated detectors consists of a Ti/Pt/Au layer on the front-side of a $500\mu\text{m}$ thick semi-insulating GaAs substrate. The back-side is an alloyed Ge/Au ohmic contact. The structure of these contacts are squares with sides of between 1.5mm and 5mm . In order to separate the behaviour of the contacts, an independent determination of those parameters of the bulk material which are responsible for a satisfactory functioning of the detector are necessary.

We present a theoretical model of the detector which simulates detector properties according to relevant parameters such as the resistivity ρ , the mobility μ of the charge carriers, the energy level E_{DD} and concentration N_{DD} of the bulk-defects and the leakage-current j_L of the device. The aim of this study is to determine these parameters experimentally and compare materials from different suppliers. The relevant parameters are then used for the detector simulation.

2 Introduction

New experiments in high energy physics, like the Large Hadron Collider (LHC) at CERN, have challenging demands on detection systems. These are high radiation resistance, high charge carrier mobility and good signal-to-noise ratio. From this point of view, GaAs seems to be a promising material to satisfy the desired requirements [1]. Starting from this point of view we investigate different semi-insulating GaAs wafers from various manufacturers.

3 Theory

The built-in potential of the Schottky contact and the applied reverse bias create an electric field within the detector. The resultant field is essentially dependent on the space charge in the depletion zone. The model of the space charge uses at present the energy levels of the flat donors and acceptors, one ionized deep donor and the charge carriers in the valence and conduction bands. This space charge and its electric field can be calculated numerically. Consequently the Poisson equation and the transport equation are involved via the quasi-Fermi level of the charge carriers during a constant current flow. A more detailed account of the model is given elsewhere [2]. The delivered electric field is the basis for calculating the charge collection efficiency according to Ramo's theorem [3]. The relevant parameters in the model and their determination methods are summarized in Tab.1.

Parameter	Method
Resistivity ρ	Resistivity mapping Hall
Mobility μ	Hall
Energy levels E_{DD}	Admittance Spectroscopy PICTS, Hall
Defect density N_{DD}	IR Spectroscopy
Current density j_L	I-V characteristics

Tab.1 Relevant parameters and their determination

Fig.1 and Fig.2 show the calculated space charge and field distributions in the detector for a bias voltage of -375V and the following input parameters: $\rho = 4.8 \cdot 10^7 \Omega\text{cm}$, $\mu = 7500\text{cm}^2/\text{Vs}$, $E_{DD} = 0.8\text{eV}$, $N_{DD} = 5 \cdot 10^{15}\text{cm}^{-3}$, $j_L = 38\text{nA/mm}^2$.

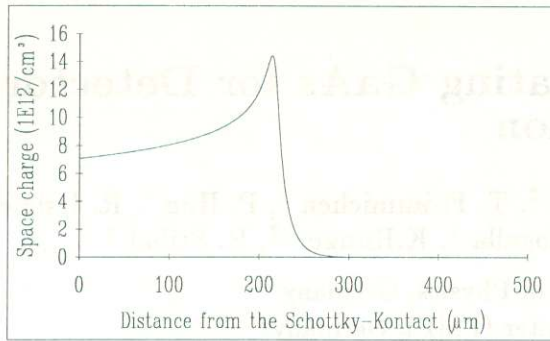


Fig.1:Space charge distribution in the detector

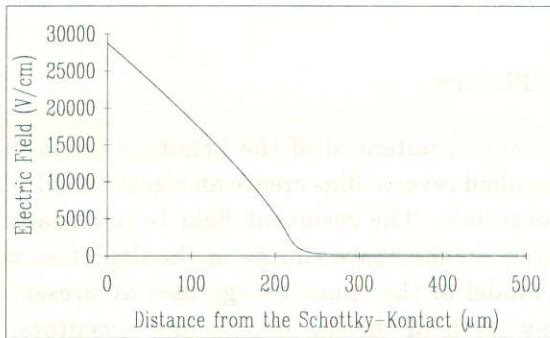


Fig.2:Electric field distribution in the detector

4 Experimental Results

4.1 Resistivity mapping

To evaluate the specific resistivity ρ and homogeneity of wafers, contactless measurements based on time-dependent charge transients were made. This method is described in detail in [4]. The investigated MCP wafers had specific resistivities between $2.5 \times 10^7 \Omega\text{cm}$ and $7 \times 10^7 \Omega\text{cm}$. The scan across the wafer showed a variation of $\pm 5\%$.

4.2 Hall measurements

The resistivity, the mobility and the carrier concentration can be determined by Hall measurements using the method described by van der Pauw [5]. Although the variation of the resistivity was less than 5% across different regions of one wafer, the variation in the mobility was greater than 15%. Temperature-dependent Hall measurements were carried out in a temperature range of between 265K and 340K to calculate the energy level of the deep donor EL2. The compensation of the shallow acceptor levels is caused by this donor being close to the middle of the bandgap. In Fig.3 the Arrhenius

plot of an investigated wafer (Wacker) is given for $-1/eR_H$ and $\ln(-eT^{3/2}R_H)$ where R_H is the measured Hall constant. In both cases the slope results in an energy level of $E_{DD} = 0.79\text{eV}$.

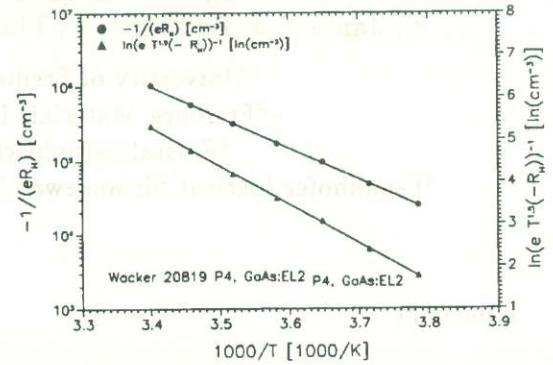


Fig.3:Arrhenius plot of a temperature dependent Hall measurement

4.3 PICTS measurements

Applied to high resistivity materials, DLTS fails as the standard method of determining deep levels because of the lack of free charge carriers. The amount of these is therefore increased by photo pulses giving photo-induced current transients (PICTS) [6]. The analysis of the temperature-dependent transients was carried out by a regularization method [7]. As can be seen in Fig.4, the PICTS spectrum shows deep levels only in the range of 0.12eV to 0.48eV below the conduction band. Levels close to the gap centre like the EL2 defect were not detected in the analysed temperature range, but are expected for higher temperatures. According to M.J.S.P. Basil and P. Motisuke [8], an increased background current at these temperatures masks the response signal of the midgap levels.

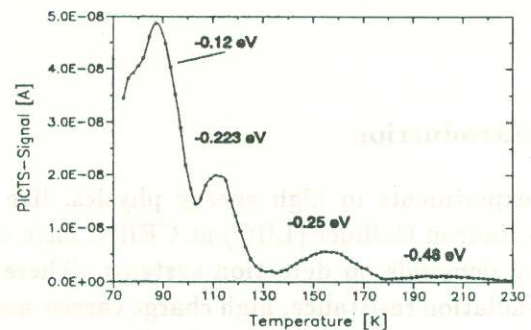


Fig.4:PICTS-spectrum of undoped si-GaAs

4.4 Admittance spectroscopy

Supplying the results of PICTS, the frequency-dependent analysis of capacitance and conductance data facilitates the analysis of levels close to the gap center. An additional contribution to the capacitance of a Schottky contact is found at the resonance frequency of the thermal activation process [9]. The relaxation times τ of the deep levels were extracted by a regularization method [10] providing a good resolution compared to conventional methods. The activation energies and capture cross-sections are obtained from the temperature dependence of the correlated maxima. Four deep centres were found close to the gap centre (Fig.5).

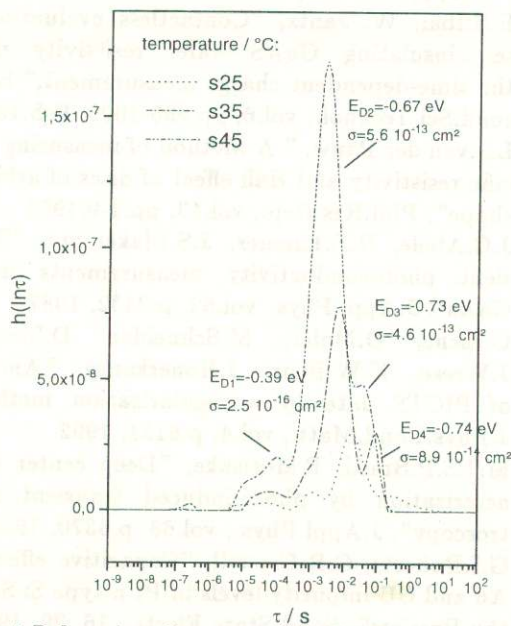


Fig.5: Relaxation time spectra at different temperatures from admittance data

4.5 IR-Spectroscopy

The EL2 concentration could be evaluated by the NIR transmission line scanning method developed by J. Windscheif et al. [11]. The method is based on a linear silicon diode array, which detects the transmitted IR intensity in the range $975 \pm 75 \text{ nm}$. This absorption band is caused mainly by the neutral EL2 defects in undoped semi-insulating GaAs. The concentrations of the different samples had been measured between $1.45 \times 10^{16} - 1.8 \times 10^{16} \text{ cm}^{-3}$.

4.6 Current-Voltage characteristics

Dark current-voltage measurements were carried out to determine the leakage current density j_L during the certain reverse bias conditions of the detector. The values of the tested wafers were between 8 nA/mm^2 and 36 nA/mm^2 at 20°C and -200 V bias voltage. Good uniformity across each wafer was observed.

4.7 Charge collection efficiency

The charge collection efficiency is defined as the ratio of the detected charge in the pre-amplifier and the generated charge in the detector. This ratio is lower than 1 because of incomplete charge collection due to trapping and incomplete depletion in the detector. To judge the detector quality of the different samples, spectra from alpha-sources (^{241}Am , ^{212}Bi , ^{212}Po) were taken and evaluated from the viewpoint of charge collection efficiency, energy resolution and signal-to-noise ratio. Table 2 summarizes the experimental results.

Wafer	Hall μ [cm^2/Vs]	Hall ρ [$10^7 \Omega \text{cm}$]	Admittance E_{DD} [eV]	PICTS E_{DD} [eV]	IR-Spectroscopy N_{DD} [10^{16} cm^{-3}]	I-V Charact. j_L (-200 V) [nA/mm^2]	α -Spectrum CCE (-200V) [%]
MCP 2266/3	5486	4.3	0.23; 0.40 0.67; 0.74		1.80	30.2	35
MCP 2266/52		1.4	0.26; 0.54 0.73	0.10; 0.18 0.36; 0.45	1.55	17.1	22
MCP 2266/102					1.72	12.1	15
Freiberg 40120/99		0.8	0.23; 0.50 0.66; 0.73		1.45	31.5	29
AXT 20227/58		6.8	0.28; 0.55 0.64; 0.73		1.61	8.9	19
Outokumpu 2331/123	5000	0.3		0.17; 0.28 0.29; 0.36	1.51	36.4	38
Wacker 20819/82	5600	4.5	0.39; 0.67 0.73; 0.74	0.12; 0.22 0.25; 0.48		38	35

Tab.2 Measured values of the different wafers

5 Conclusion

As predicted by the model, the *cce* increases with increasing leakage current j_L . This can be explained by an increased carrier concentration in the conduction band which lowers the space charge and rises the depletion width (Fig.6). The increase in *cce* with the leakage current has to be paid against a lack of energy resolution of the detector. Al-

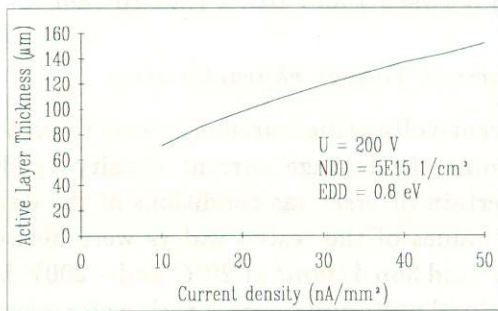


Fig.6: Calculated depletion width vs. leakage current density

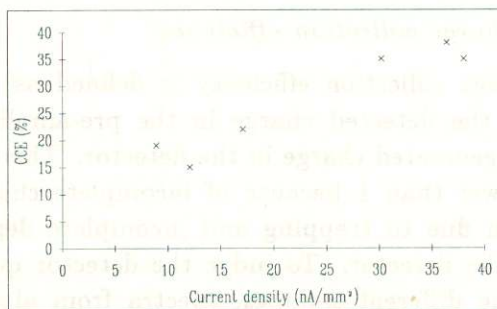


Fig.7: Measured charge collection efficiency vs. leakage current density j_L

though the used model takes into account only a three level scheme, the calculated *cce* vs. bias voltage according to the theorem of Ramo shows good equivalence to the measured values (Fig.8). Nevertheless, a more detailed model should take into account all the other measured energy levels.

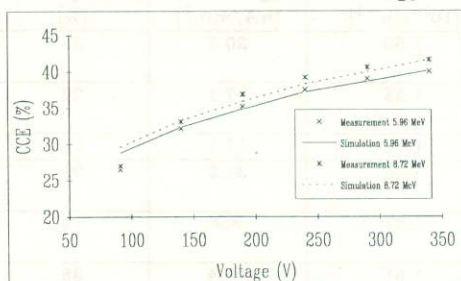


Fig.8: Charge collection efficiency vs. bias voltage

References

- [1] K.W.Benz, R.Irsigler, J. Ludwig, J.Rosenzweig, K.Runge, F.Schäfer, J. Schneider, M.Webel, "X-ray detectors based on semi-insulating GaAs substrate", Nucl.Instr.a.Meth., vol.A322, pp.493-498, 1992
- [2] M.Rogalla, J.Chen, P.Edwards, T.Frömmichen, R.Geppert, R.Irsigler, T.Kleindienst, M.Kohler, J.Ludwig, J.Pfister, T.Plötze, K.Runge, F.Schäfer, T.Schmid, "Calculation of the electric field in GaAs detectors", submitted for publication in Nucl.Instr.a.Meth.
- [3] G.Cavalleri, E.Gatti, G.Fabri, "Extension of Ramos theorem as applied to induced charge in semiconductor detectors", Nucl.Instr.a.Meth., vol.92, pp.137-141, 1971
- [4] R.Stibal, W. Jantz, "Contactless evaluation of semi-insulating GaAs wafer resistivity using the time-dependent charge measurement", Semicond.Sci.Technol., vol.6, pp.995-1000, Feb.1991
- [5] L.J.van der Pauw, "A Method of measuring specific resistivity and Hall effect of discs of arbitrary shape", Phil.Res.Rep., vol.13, pp.1-9,1958
- [6] J.C.Abele, R.E.Kremer, J.S.Blakemore, "Transient photoconductivity measurements in si-GaAs", J.Appl.Phys. vol.62, p.2432, 1987
- [7] C.Eiche, D.Maier, M.Schneider, D.Sinerius, J.Weese, K.W.Benz, J.Honerkamp, "Analysis of PICTS data by a regularization method", J.Phys.Cond.Matt., vol.4, p.6131, 1992
- [8] M.J.S.P.Brasil, P.Motisuke, "Deep center characterization by photo-induced transient spectroscopy", J.Appl.Phys., vol.68, p.3370, 1990
- [9] G.I.Roberts, C.R.Crowell, "Capacitive effects of Au and CU impurity levels in Pt n-type Si Schottky Barriers", Solid State Electr., 16, 29, 1973
- [10] C. Eiche, M.Fiederle, J.Weese, D.Maier, D.Ebling, J.Ludwig, K.W.Benz, "Analysis of deep levels in GaAs detector diodes using impedance spectroscopy", Mat.Res.Soc.Symp.Proc. 302, 375, 1993
- [11] J.Windscheif, M.Baeumler, U.Kaufmann, "New quantitative line scanning technique for homogeneity assessment of semi-insulating GaAs wafers", Appl.Phys.Lett., vol.46, no.7, pp.661-663